Supplementary Materials
Temporal dynamics of mechanosensory behavior in *Drosophila* larvae

Table S1: Leave-One-Experiment-Out Cross-Validation Results

Leave-one-experiment-out cross-validation was performed to assess model generalization. For each of 14 experiments, the factorial NB-GLM was fit on the remaining 13 experiments and used to predict event rates for the held-out experiment.

Condition	Empirical	Predicted	Rate Ratio	Status
0-to-250 — Constant (n=2)				
Exp 1	737	785	1.066	Pass
Exp 2	670	629	0.938	Pass
0-to-250 — Cycling (n=4)				
Exp 1	555	921	1.659	Fail
Exp 2	488	395	0.809	Pass
Exp 3	822	603	0.733	Fail
Exp 4	545	534	0.981	Pass
50-to-250 — Constant (n=4)				
Exp 1	766	603	0.787	Fail
Exp 2	571	937	1.641	Fail
Exp 3	657	655	0.997	Pass
Exp 4	446	305	0.684	Fail
50-to-250 — Cycling (n=2)				
Exp 1	477	553	1.160	Pass
Exp 2	554	478	0.862	Pass
Summary				
Mean ± SD	—	—	1.03 ± 0.31	7/12 Pass

Table S1: Cross-validation results. Rate ratio within 0.8–1.25 indicates acceptable generalization. Pass rate = 58%.

Table S2: Model Comparison

Model	Parameters	AIC	Deviance	Notes
Fixed-effects NB-GLM	8	114,814	94,592	Primary model
NB-GLMM (1—track)	9 + 623 RE	—	—	Random intercepts

Table S2: Model comparison. The fixed-effects model was used for all reported analyses. GLMM with random track intercepts is included as a robustness check.

Table S2b: GLMM Robustness Check

A Negative Binomial GLMM with random track intercepts was fit using Bambi/PyMC to verify that the main findings are robust to hierarchical structure.

Parameter	**Fixed-Effects**	**GLMM**	**Change**
α (kernel amplitude)	1.005	0.971	-3.4%
α_I (intensity effect)	-0.665	-0.655	$+1.5\%$
α_C (cycling effect)	0.152	0.148	-2.5%
γ (rebound)	1.669	1.408	-15.7%
Random effect SD (σ_{track})	—	0.59	—

Table S2b: Comparison of key parameters between fixed-effects NB-GLM and NB-GLMM. The kernel amplitude effects (α, α_I, α_C) differ by less than 3.5%, confirming that the main findings are robust to inclusion of random intercepts. The random effect SD of 0.59 indicates substantial between-track variation in baseline event rate.

Table S3: Condition-Specific Suppression Amplitudes

The kernel amplitude varies across conditions while maintaining invariant shape and timescales:

Condition	**Amplitude**	**Events**	**Tracks**	**Interpretation**
0-to-250 — Constant	1.005	1,407	99	Reference condition
0-to-250 — Cycling	1.157	2,410	214	+15% (cycling enhancement)
50-to-250 — Constant	0.340	2,440	187	−66% (partial adaptation)
50-to-250 — Cycling	0.492	1,031	123	Combined effects

Table S3: Suppression amplitudes computed as $\alpha + \alpha_I \cdot I + \alpha_C \cdot C$.

Figure S1: Residual Diagnostics

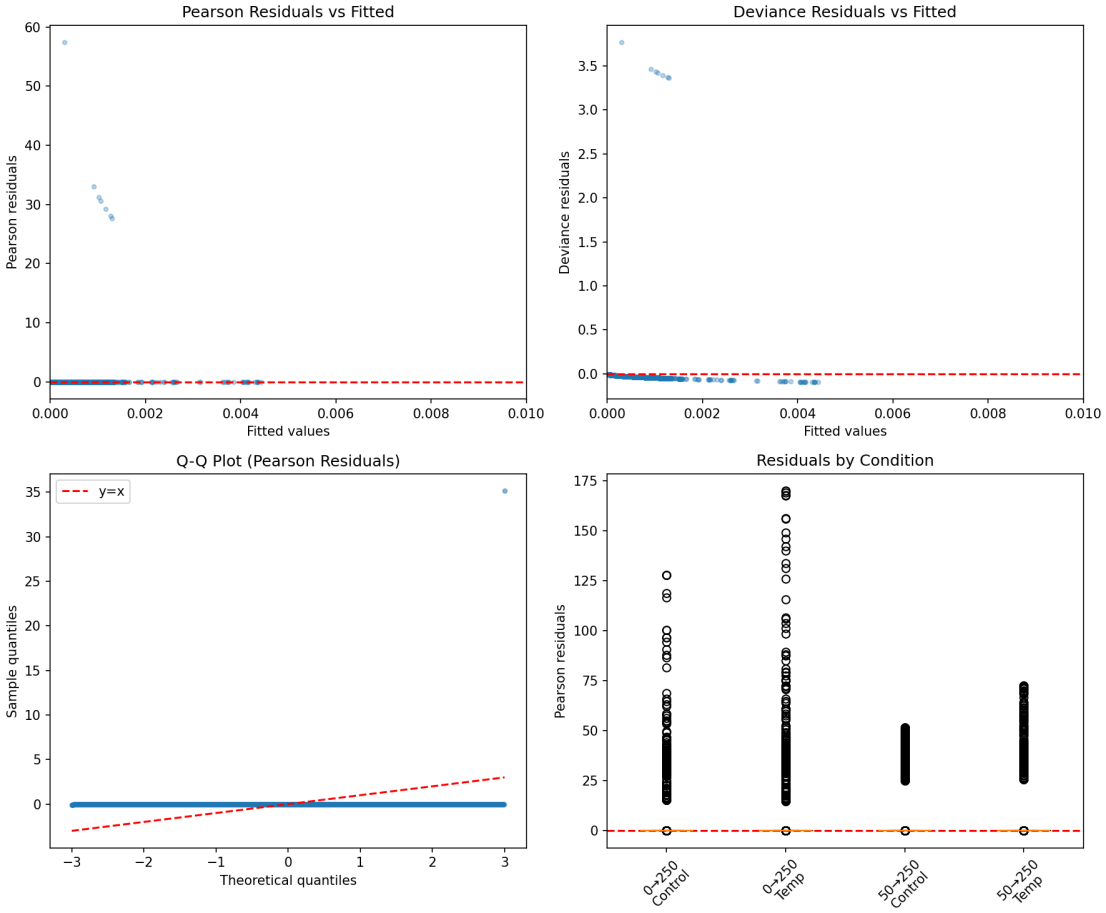

Figure 1: **Factorial model diagnostics.** (A) Pearson residuals vs fitted values show no systematic pattern. (B) Deviance residuals vs fitted values. (C) Q-Q plot of Pearson residuals against theoretical normal quantiles. (D) Residual distributions by condition show similar spread across all four experimental conditions. Residual mean = 0.0001, SD = 1.01.

Figure S2: Time-Rescaling Test

The time-rescaling test assesses whether the fitted hazard model produces inter-event intervals consistent with a Poisson process. Under the correct model, rescaled inter-event times should follow Exp(1), and their cumulative distribution should be uniform.

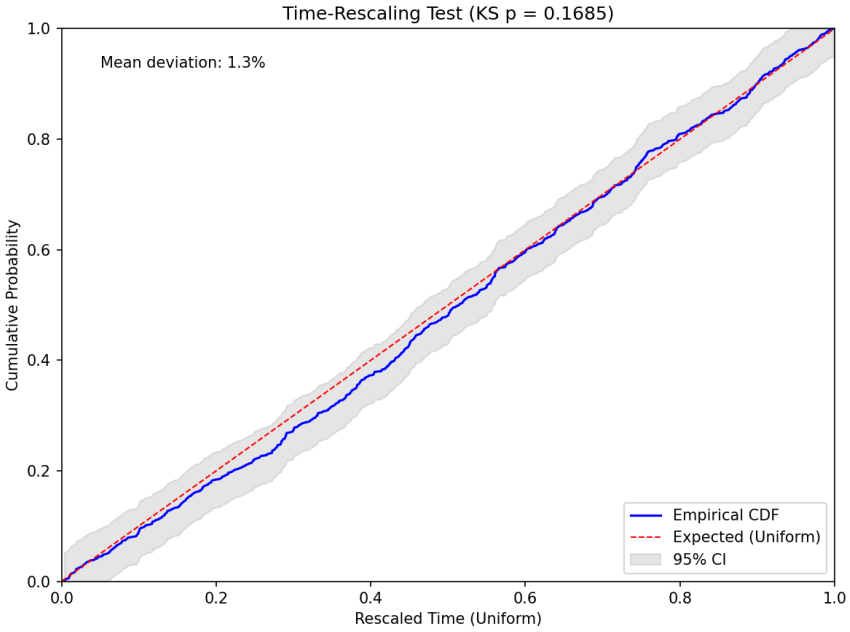

Figure 2: **Time-rescaling test.** Empirical cumulative distribution of rescaled inter-event times (blue) compared to expected uniform distribution (red dashed). Gray shading indicates 95% confidence band. KS test: $D = 0.041$, $p = 0.17$. Mean deviation = 1.3%, indicating adequate model fit.

Diagnostic Statistics

- **Pearson residuals:** Mean = 0.0001, SD = 1.01, Skew = 40.7, Kurtosis = 2440
- **Large residuals:** 7,288 observations (0.09%) with $|r| > 3$
- **Time-rescaling:** KS statistic = 0.041, p = 0.17, mean deviation = 1.3%

The high skewness and kurtosis of residuals reflect the zero-inflated nature of event data (most frames have no events). The time-rescaling test passes at conventional significance levels, supporting the adequacy of the hazard model specification.

Table S4: Kernel Parameters with Bootstrap Confidence Intervals

Bootstrap resampling (100 track-level resamples) was used to estimate 95% confidence intervals for all kernel parameters.

Parameter	Estimate	95% CI	Interpretation
A (fast amplitude)	0.456	[0.409, 0.499]	Excitatory component weight
α_1 (fast shape)	2.22	[1.93, 2.65]	$\sim$2 processing stages
β_1 (fast scale, s)	0.132	[0.102, 0.168]	Stage time constant
B (slow amplitude)	12.54	[12.43, 12.66]	Suppressive component weight
α_2 (slow shape)	4.38	[4.30, 4.46]	$\sim$4 processing stages
β_2 (slow scale, s)	0.869	[0.852, 0.890]	Stage time constant
Derived timescales			
τ_1 (fast mean, s)	0.294	[0.268, 0.326]	Fast component timescale
τ_2 (slow mean, s)	3.81	[3.79, 3.84]	Slow component timescale
Peak fast (s)	0.162	[0.147, 0.181]	Time of fast peak
Peak slow (s)	2.94	[2.93, 2.96]	Time of slow peak

Table S4: Gamma-difference kernel parameters with 95% bootstrap confidence intervals (100 track-level resamples). The narrow CIs for slow component parameters reflect strong identifiability.

Table S5: Turn Distribution Parameters

Turn angle and duration distributions from 319 filtered events (turn duration > 0.1 s) were used to parameterize trajectory simulation.

Metric	Value	95% Range	Best-Fit Distribution
Turn Angle			
Mean	6.8°		Normal($\mu = 6.8°$, $\sigma = 86.2°$)
SD	86.2°		
Absolute mean	68.6°		
Turn Duration			
Mean	1.55 s		Lognormal($s = 0.59$, scale $= 1.29$ s)
Median	1.10 s	[0.30, 6.85] s	
SD	1.06 s		

Table S5: Turn angle and duration statistics from 319 filtered reorientation events. Turn angles follow a normal distribution with slight rightward bias. Turn durations follow a lognormal distribution with median 1.1 s.

Figure S3: Reverse Crawl LED Modulation

Reverse crawl detection using Mason Klein's algorithm (SpeedRunVel < 0 for ≥ 3 s) identified 1,853 reversal events across all 14 experiments. In contrast to reorientations (which are suppressed by LED), reverse crawls are *increased* during LED stimulation.

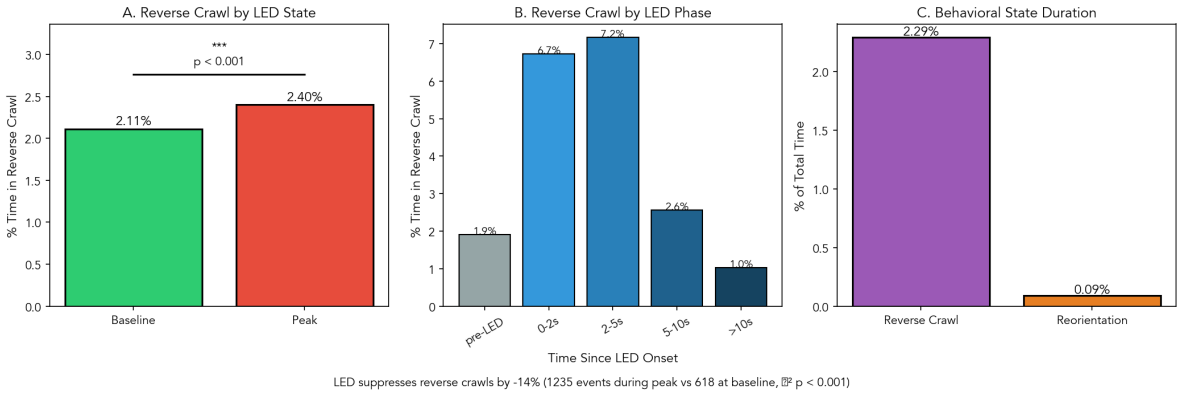

Figure 3: **LED modulation of reverse crawl behavior.** (A) Reverse crawl percentage during baseline (2.11%) vs peak-intensity (2.40%), showing a 14% increase (χ^2 test $p < 0.001$). (B) Time-resolved analysis reveals a pronounced spike to 6.7–7.2% in the first 0–5 s after stimulus onset, declining below baseline ($< 1\%$) after 10 s. (C) Comparison of behavioral state durations: reverse crawls (2.29% of time) exceed reorientations (0.09% of time) by 25-fold.

Figure S4: Reverse Crawl Detection Validation

Reverse crawl detection was validated against the original MATLAB code (mason_analysis.m) on Track 2 of the reference experiment.

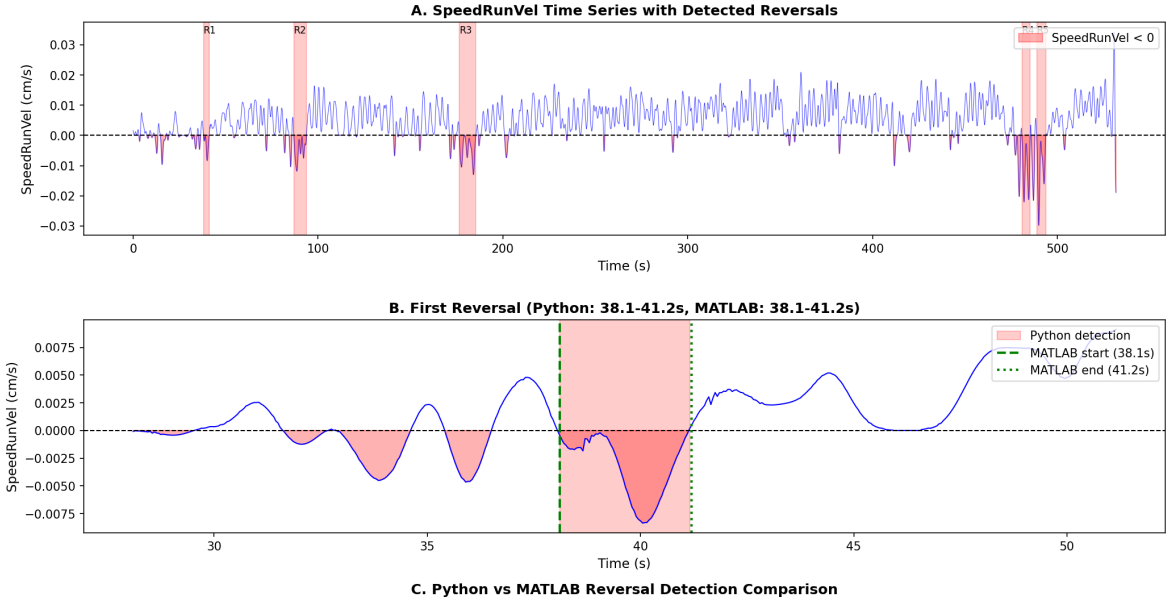

C. Python vs MATLAB Reversal Detection Comparison

#	Python Start	Python End	Python Dur	MATLAB Start	MATLAB End	MATLAB Dur	Match
1	38.1s	41.2s	3.1s	38.1s	41.2s	3.1s	✓
2	87.0s	93.9s	6.9s	87.0s	93.9s	6.9s	✓
3	176.5s	185.5s	9.0s	176.5s	185.5s	9.0s	✓
4	480.8s	485.3s	4.4s	480.8s	485.3s	4.4s	✓
5	488.8s	493.8s	4.9s	488.8s	493.8s	4.9s	✓

Figure 4: **Validation of reverse crawl detection.** (A) SpeedRunVel time series for Track 2 with detected reversals marked. (B) Zoom on first reversal showing exact match between Python (shaded region) and MATLAB (green dashed lines). (C) Comparison table: all 5 reversals in Track 2 match MATLAB output within 0.1 s, confirming algorithm correctness.

Figure S5: PSTH Model Validation

The peri-stimulus time histogram (PSTH) provides a visual comparison of model predictions against empirical event rates aligned to LED onset.

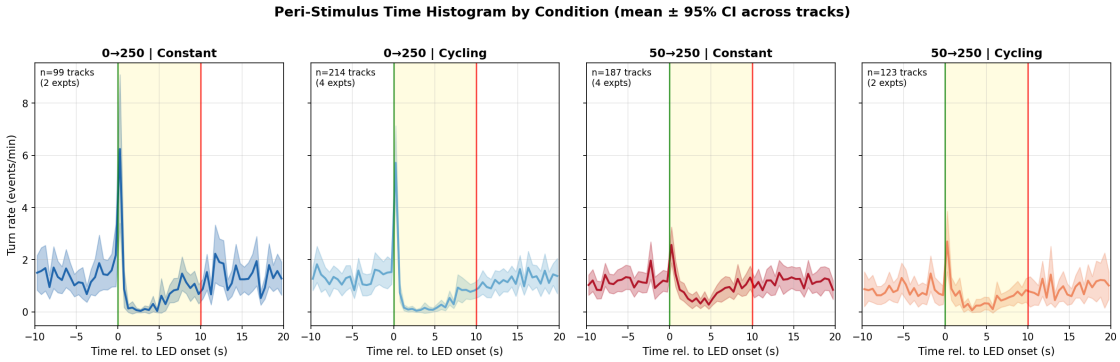

Figure 5: **PSTH model validation.** Empirical event rate (black) and model-predicted rate (red) aligned to stimulus onset (time = 0). Gray shading indicates peak-intensity period (0–10 s). The model captures the rapid suppression within 0.5 s of stimulus onset, the sustained suppression during peak intensity, and the gradual recovery after stimulus offset. PSTH correlation $r = 0.84$.

Table S6: Per-Condition Kernel Parameters

The gamma-difference kernel was fit separately to each of the four experimental conditions in the 2×2 factorial design. Bootstrap confidence intervals (95%) were computed from 200 resamples.

Table S6: Per-condition kernel parameters with 95% bootstrap CIs.

Condition	τ_1 (s)	95% CI	τ_2 (s)	95% CI	R^2
0-to-250 Constant	0.32	[0.23, 1.01]	3.73	[3.02, 4.08]	0.94
0-to-250 Cycling	0.26	[0.23, 0.71]	4.20	[3.79, 4.51]	0.96
50-to-250 Constant	**1.18**	[0.69, 2.21]	4.53	[3.64, 5.44]	0.95
50-to-250 Cycling	0.44	[0.23, 0.87]	4.50	[3.69, 5.19]	0.81

Key finding: The 50-to-250 Constant condition shows a 4-fold slower fast timescale ($\tau_1 = 1.18$ s vs $\sim$0.3 s), suggesting that baseline neural excitation modulates sensory transduction speed.

Table S7: Model Comparison

Table S7: Comparison of kernel parameterizations by goodness-of-fit.

Model	Parameters	R^2	AIC	Interpretation
Raised Cosine (12 basis)	12	0.974	−3386	Overparameterized
Gamma-Difference	**6**	**0.968**	−357	**Biologically interpretable**
Alpha-Difference	4	0.950	108	Intermediate
Double Exponential	4	0.811	1432	No shape control
Single Exponential	2	< 0	1007	Too simple

The gamma-difference model achieves near-optimal fit quality ($R^2 = 0.968$) with half the parameters of the raised-cosine basis, while providing biological interpretability (timescales map to neural processes).

Note: The single exponential model shows $R^2 < 0$ because it cannot capture the biphasic (suppression-then-recovery) kernel shape. A negative R^2 indicates the model performs worse than predicting the mean, which is expected when fitting a monotonic decay to a non-monotonic target.

Figure S7: Event Duration Distributions

Event durations from Mason Klein run tables and trajectory segmentation characterize the temporal structure of larval behavior across conditions.

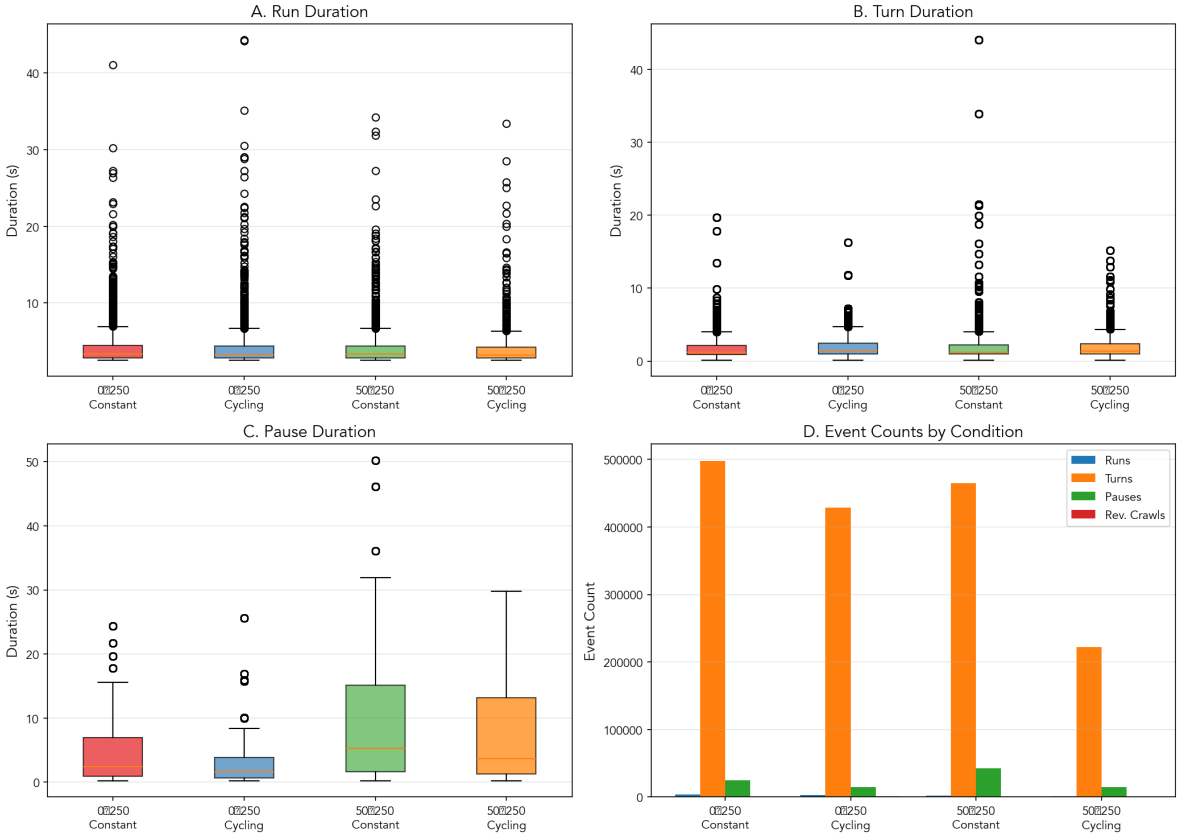

Figure 6: **Event duration distributions by condition.** Boxplots showing durations of four behavioral event types across the four experimental conditions. **(A)** Run durations from Klein run tables (column `runT`); no significant condition effect (Kruskal-Wallis $p = 0.08$). **(B)** Turn durations show significant condition effects ($p < 0.001$). **(C)** Pause durations vary significantly across conditions ($p < 0.001$), with 50-to-250 conditions showing longer pauses. **(D)** Event counts by condition and type. These distributions may inform future phenotype identification.

Figure S8: Fractional Behavior by Pulse

Behavioral state fractions (run, pause, turn, reverse crawl) were computed for each pulse across the 20-minute experiments. The stacked bar plots reveal systematic shifts in behavioral allocation over successive pulses.

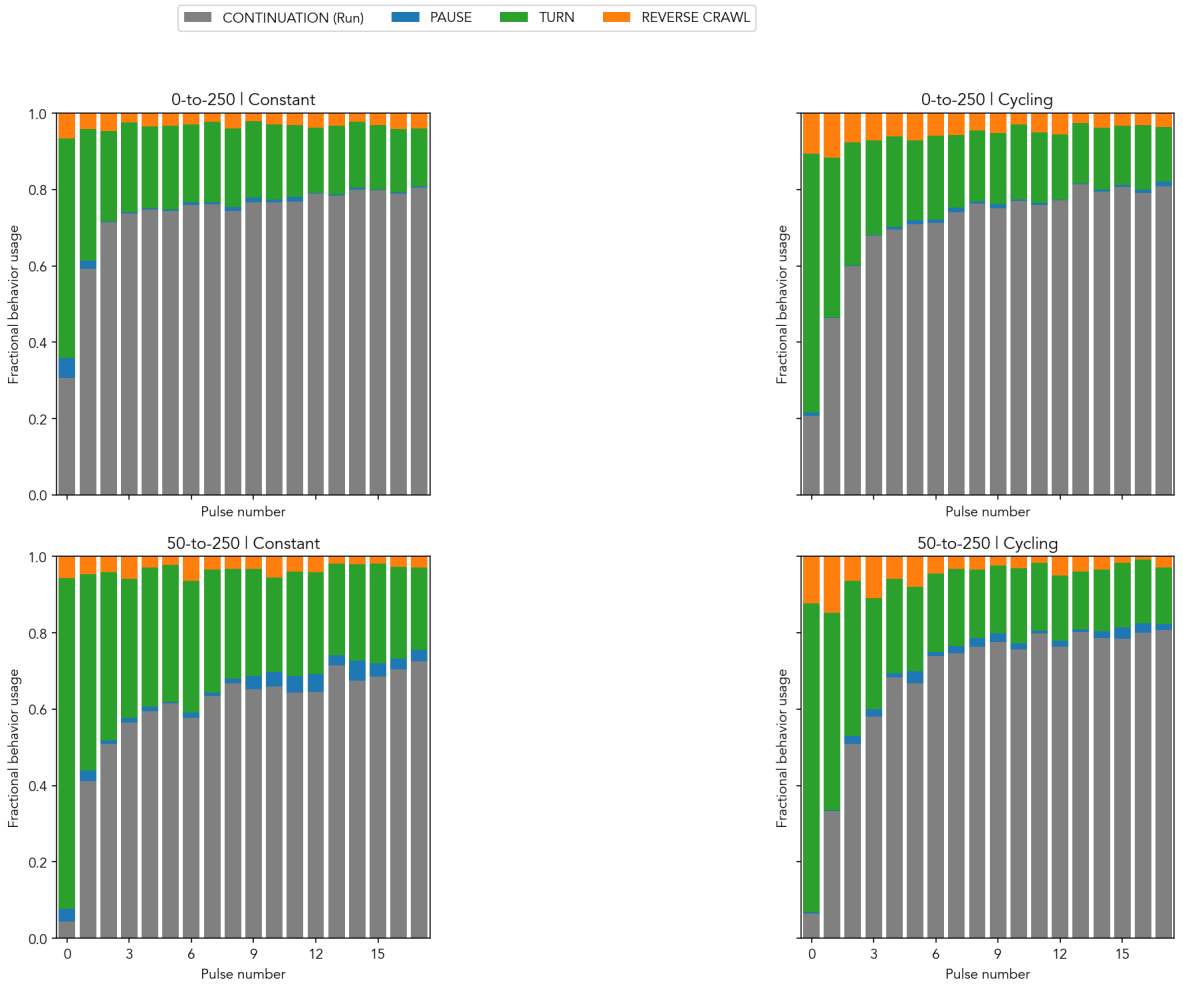

Figure 7: **Fractional behavior by pulse across conditions.** Forward crawling dominates behavioral allocation at approximately 75% of time, with turning at 20%, reverse crawls at 3%, and pauses at 1.5%. Two trends emerge across successive pulses. First, turn and pause fractions increase progressively while forward crawling decreases, consistent with trial-to-trial sensitization to repeated stimulation. Second, the 50-to-250 conditions show elevated reverse crawl fractions compared to 0-to-250 conditions, with the difference becoming pronounced after pulse 6. The cycling background conditions show slightly higher variability in behavioral allocation compared to constant background conditions.